Journal of Engineering Mathematics **28:** 427–445, 1994.

The onset of steady Marangoni convection in a spherical geometry

S.K. WILSON
Department of Mathematics, University of Strathclyde, Livingstone Tower, 26 Richmond Street, Glasgow G1 1XH UK

Received September 1992; accepted in revised form November 1993

Abstract. In this paper we use a combination of analytical and numerical techniques to analyse the onset of steady Marangoni convection in a spherical shell of fluid with an outer free surface surrounding a rigid sphere. In so doing we correct the formulation of the problem and the results presented by Cloot & Lebon (*Microgravity sci. technol.* **3** (1) 1990 : 44-46). We find that if the free surface of the layer is non-deformable then the layer is always stable when heated from the outside and is unstable when heated from the inside if the magnitude of the (positive) non-dimensional Marangoni number is sufficiently large. If the free surface of the layer is deformable then the layer is always unstable when heated from the inside. It is stable when heated from the outside if $C_r < r_2/4$, but if $C_r > r_2/4$ then it is unstable if the magnitude of the (negative) Marangoni number is sufficiently large, where C_r is the non-dimensional Crispation number and r_2 the non-dimensional radius of the undisturbed outer free surface of the fluid.

1. Introduction

The aim of this paper is to describe the onset of steady Marangoni convection in a spherical shell of fluid with an outer free surface surrounding a rigid sphere.

A great deal of work has been performed to investigate the onset of Marangoni convection in a planar layer, beginning with the pioneering contribution of Pearson [8]. He showed that if the layer is heated from below and the upper free surface is non-deformable then it is unstable to steady Marangoni convection driven by surface tension gradients when a suitably defined non-dimensional Marangoni number exceeds a critical value. Scriven & Sternling [12] relaxed the restriction of a non-deformable free surface and found that including capillary waves at the free surface has a dramatic destabilising effect on the layer, and Smith [13] showed that including gravity waves as well has a stabilising effect on long wavelength disturbances. The layer is always stable to steady Marangoni convection when heated from above. Takashima [14,15] performed extensive numerical calculations for the onset of both steady and overstable convection, and more recently Gouesbert *et al.* [4] have generalised his work.

By contrast much less work has been done on the onset of Marangoni convection in a spherical geometry. The first paper on the subject of which the author is aware is that by Pirotte & Lebon [9] who followed the approach taken by Chandrasekhar [1, Chap. VI] for the related problem of buoyancy-driven convection in a spherical geometry, and calculated critical values of the Marangoni number for the onset of steady convection in the simplest case when the outer free surface of the fluid is non-deformable. Hoefsloot & Hoogstraten [5] solved the same problem but obtained different critical values for the Marangoni number, an inconsistency which was resolved by Pirotte & Lebon [10] who identified a mistake in the non-dimensionalisation in their earlier work. Once this error was corrected the results from the two papers are in agreement. Both works treated both isothermal and constant heat

flux thermal boundary conditions at the inner boundary. Cloot & Lebon [2] extended the earlier work of Pirotte & Lebon [9,10] to include the effects of a deformable free surface. Unfortunately, they made a number of errors in the formulation of the boundary conditions for the problem, with the consequence that the interesting bifurcation behaviour they describe needs to be re-examined. Recently Lebon, Dauby & Cloot [7] have reviewed the work on this problem.

In this paper we shall investigate the onset of steady Marangoni convection in a spherical geometry with a deformable free surface. The work extends that of Pirotte & Lebon [9,10] and Hoefsloot & Hoogstraten [5] and extends and corrects that of Cloot & Lebon [2].

2. Problem formulation

The basic geometry we wish to examine is that of a spherical shell of quiescent fluid with an outer free surface of radius R_2 and temperature T_2 about a rigid sphere of radius $R_1 < R_2$ and temperature T_1. The sphere is surrounded by a passive gas at temperature T_∞ and pressure P_∞, and for convenience we define $d = R_2 - R_1$ to be the thickness of the undisturbed shell of fluid.

Subject to the Boussinesq approximation and neglecting the effect of gravity entirely the governing equations for an incompressible fluid with velocity $\mathbf{U}$, temperature T and pressure P are

$$\frac{\partial \mathbf{U}}{\partial t} + (\mathbf{U} \cdot \nabla)\mathbf{U} = -\frac{1}{\rho}\nabla P + \nu \nabla^2 \mathbf{U}, \tag{1}$$

$$\frac{\partial T}{\partial t} + \mathbf{U} \cdot \nabla T = \kappa \nabla^2 T \tag{2}$$

$$\nabla \cdot \mathbf{U} = 0, \tag{3}$$

where the constants ρ, ν and κ represent the density, kinematic viscosity and thermal diffusivity of the fluid respectively. The fluid motion (if any) is driven entirely by the thermocapillary effect at the outer free surface, where the surface tension τ is taken to be dependent on the temperature T according to the simple linear law $\tau = \tau_0 - \gamma(T - T_2)$, where the constant τ_0 is the value of τ in the undisturbed state and the constant γ is positive for normal fluids. At the outer free surface the usual conditions of continuity of normal and tangential stress hold and the temperature obeys Newton's law of cooling, viz.

$$-k\frac{\partial T}{\partial \mathbf{n}} = h(T - T_\infty),$$

where k is the thermal conductivity of the fluid, h is the heat transfer coefficient between the free surface and the gas and $\mathbf{n}$ is the outward unit normal to the free surface. At the inner boundary in addition to the usual no slip boundary condition for the fluid velocity we consider two different thermal boundary conditions. Either the temperature of the boundary is held constant at T_1 (the so called "conducting" boundary condition) or the heat flux is held constant (the so called "insulating" boundary condition).

To simplify the analysis we introduce non-dimensional variables. Taking the scales for length, time, velocity and temperature to be d, d^2/κ, κ/d and $(T_1 - T_2)$ respectively and non-dimensionalising the equations and boundary conditions gives rise to five non-dimensional

groups, namely the *Prandtl number* $P_r = \nu/\kappa$, the *Marangoni number* $M = \gamma(T_1 - T_2)d/\rho\nu\kappa$, the *Crispation number* $C_r = \rho\nu\kappa/\tau_0 d$, the Biot number $B_i = hd/k$ and the non-dimensional radius of the rigid sphere $r_1 = R_1/d$. The non-dimensional radius of the undisturbed free surface $r_2 = R_2/d$ is given by $r_2 = r_1 + 1$. Note that if the layer is heated from the inside then $T_1 > T_2$ and so $M > 0$ while if the layer is heated from the outside then $T_1 < T_2$ and so $M < 0$. Hereafter all quantities will be non-dimensional unless stated otherwise.

To describe the situation we choose spherical polar co-ordinates (r, θ, ϕ) with their origin at the centre of the rigid sphere $r = r_1$. In the undisturbed state the free surface is at $r = r_2$, and when motion occurs it will be deformed and then we denote its position by $r = r_2 + F(\theta, \phi, t)$. The equations and boundary conditions admit a solution in which the fluid is at rest, $\mathbf{U} = \mathbf{U}_0 = \mathbf{0}$, the temperature is given by $T = T_0(r) = \alpha/r + \beta$ where $\alpha = r_1 r_2$ and $\beta = r_2 T_2 - r_1 T_1$, the pressure is constant, $P = P_0 = P_\infty + 2P_r/r_2 C_r$, and the free surface is undeformed, $F = F_0 = 0$. In what follows we shall investigate the linear stability of perturbations to this basic state.

3. Linearised Problem

We analyse the linear stability of the basic state in the usual manner by seeking perturbed solutions in the form

$$\mathbf{U} = \mathbf{U}_0 + \mathbf{U}_1, \quad T = T_0 + T_1, \quad P = P_0 + P_1, \quad F = F_0 + F_1,$$

where $\mathbf{U}_1 = (u_r, u_\theta, u_\phi)$. Substituting these forms into the governing equations (1) - (3) and neglecting second order and higher terms in the perturbation quantities we obtain the linearised equations

$$\left(\nabla^2 - \frac{1}{P_r}\frac{\partial}{\partial t}\right)\mathbf{U}_1 = \frac{1}{P_r}\nabla P_1, \tag{4}$$

$$\left(\nabla^2 - \frac{\partial}{\partial t}\right)T = -\frac{\alpha}{r^2}u_r, \tag{5}$$

$$\nabla \cdot \mathbf{U}_1 = 0. \tag{6}$$

To eliminate P_1 we take the curl of equation (4) twice and use equation (6) to yield the equation

$$\nabla^2\left[\nabla^2 - \frac{1}{P_r}\frac{\partial}{\partial t}\right](ru_r) = 0 \tag{7}$$

for u_r derived by Chandrasekhar [1, Chap VI]. For convenience we define the operator L^2 by

$$L^2 = -\left[\frac{1}{\sin\theta}\frac{\partial}{\partial\theta}\left(\sin\theta\frac{\partial}{\partial\theta}\right) + \frac{1}{\sin^2\theta}\frac{\partial^2}{\partial\phi^2}\right] \tag{8}$$

so that we can write

$$\nabla^2 = \frac{1}{r^2}\frac{\partial}{\partial r}\left(r^2\frac{\partial}{\partial r}\right) - \frac{1}{r^2}L^2.$$

The linearised version of the kinematic boundary condition at the free surface $r = r_2 + F_1$ is given by

$$\frac{\partial F_1}{\partial t} - u_r = 0 \tag{9}$$

evaluated on $r = r_2$. The condition of continuity of normal stress across the free surface takes the form

$$[\mathbf{n} \cdot \mathbf{T} \cdot \mathbf{n}]_-^+ = \frac{P_r}{C_r} K\tau \tag{10}$$

where $[\ldots]_-^+$ denotes the jump across the free surface, $\mathbf{T}$ is the stress tensor in the fluid, $\mathbf{n}$ is the unit outward normal at the free surface and K is the curvature of the free surface. Neglecting second order and higher quantities in the perturbation quantities we have

$$\mathbf{n} = \left(1, -\frac{1}{r}\frac{\partial F_1}{\partial \theta}, -\frac{1}{r\sin\theta}\frac{\partial F_1}{\partial \phi}\right), \quad K = \nabla \cdot \mathbf{n} = \frac{2}{r_2} - \frac{(2 - L^2)F_1}{r_2^2}.$$

At leading order equation (10) yields $-P_\infty + P_0 = 2P_r/rC_r$ evaluated on $r = r_2$ and hence $P_0 = P_\infty + 2P_r/r_2C_r$, while at first order we obtain

$$P_1 - 2P_r\frac{\partial u_r}{\partial r} = -\frac{P_r}{C_r}\left[\frac{2MC_r}{r}\left(T_1 - \frac{\alpha F_1}{r^2}\right) + \frac{(2 - L^2)F_1}{r^2}\right] \tag{11}$$

evaluated on $r = r_2$. Using equation (4) we can show that

$$L^2 P_1 = P_r\frac{\partial}{\partial r}\left[r\left(\nabla^2 - \frac{1}{P_r}\frac{\partial}{\partial t}\right)(ru_r)\right], \tag{12}$$

and so applying the operator L^2 to the boundary condition (11) and using equation (12) to eliminate L^2P_1 we obtain

$$\frac{\partial}{\partial r}\left[r\left(\frac{\partial^2}{\partial r^2} + \frac{2}{r}\frac{\partial}{\partial r} - \frac{3}{r^2}L^2 - \frac{1}{P_r}\frac{\partial}{\partial t}\right)(ru_r)\right]$$
$$+ L^2\left[\frac{2M}{r}\left(T_1 - \frac{\alpha F_1}{r^2}\right) + \frac{(2 - L^2)F_1}{r^2 C_r}\right] = 0, \tag{13}$$

evaluated on $r = r_2$. The conditions of continuity of tangential stress at the free surface take the forms

$$\mathbf{t}_\theta \cdot \mathbf{T} \cdot \mathbf{n} = -M\,\mathbf{t}_\theta \cdot \nabla T, \quad \mathbf{t}_\phi \cdot \mathbf{T} \cdot \mathbf{n} = -M\,\mathbf{t}_\phi \cdot \nabla T, \tag{14}$$

where $\mathbf{t}_\theta$ and $\mathbf{t}_\phi$ are orthonormal tangent vectors to the free surface in the θ- and ϕ-directions respectively. Neglecting second order and higher quantities in the perturbation quantities we have

$$\mathbf{t}_\theta = \left(\frac{1}{r}\frac{\partial F_1}{\partial \theta}, 1, 0\right), \quad \mathbf{t}_\phi = \left(\frac{1}{r\sin\theta}\frac{\partial F_1}{\partial \phi}, 0, 1\right),$$

and so at first order the tangential stress conditions yield

$$r\frac{\partial}{\partial r}\left(\frac{u_\theta}{r}\right) + \frac{1}{r}\frac{\partial u_r}{\partial \theta} = -\frac{M}{r}\left[\frac{\partial T_1}{\partial \theta} - \frac{\alpha}{r^2}\frac{\partial F_1}{\partial \theta}\right], \tag{15}$$

$$\frac{1}{r\sin\theta}\frac{\partial u_r}{\partial \phi} + r\frac{\partial}{\partial r}\left(\frac{u_\phi}{r}\right) = -\frac{M}{r\sin\theta}\left[\frac{\partial T_1}{\partial \phi} - \frac{\alpha}{r^2}\frac{\partial F_1}{\partial \phi}\right] \tag{16}$$

evaluated on $r = r_2$. We can combine these two equations to obtain the single condition

$$\frac{\partial}{\partial r}\left[\frac{1}{r^2}\frac{\partial}{\partial r}(r^2 u_r)\right] + \frac{1}{r^2}L^2\left[M\left(T_1 - \frac{\alpha F_1}{r^2}\right) + u_r\right] = 0, \tag{17}$$

which we can also write in the form

$$\left[\frac{\partial^2}{\partial r^2} - \frac{(2-L^2)}{r^2}\right](r u_r) + \frac{M}{r}L^2\left(T_1 - \frac{\alpha F_1}{r^2}\right) = 0 \tag{18}$$

evaluated on $r = r_2$. At first order Newton's law of cooling yields the condition

$$\frac{\partial T_1}{\partial r} + \frac{2\alpha F_1}{r^3} + B_i\left(T_1 - \frac{\alpha F_1}{r^2}\right) = 0 \tag{19}$$

evaluated on $r = r_2$. At the inner boundary $r = r_1$ the no slip condition means that $u_r = u_\theta = u_\phi = 0$ and hence, using equation (6), that $\partial(r u_r)/\partial r = 0$. The conducting boundary condition yields $T_1 = 0$ and the insulating boundary condition $\partial T_1/\partial r = 0$ evaluated on $r = r_1$.

4. Solution of the linearised problem

Motivated by the form of the operator L^2 we seek solutions in the form

$$r u_r = w(r) Y_l^m(\theta, \phi) e^{\sigma t}, \tag{20}$$

$$T_1 = T(r) Y_l^m(\theta, \phi) e^{\sigma t}, \tag{21}$$

together with

$$F_1 = F Y_l^m(\theta, \phi) e^{\sigma t}, \tag{22}$$

where $Y_l^m(\theta, \phi)$ are the spherical surface harmonics $Y_l^m(\theta, \phi) = P_l^m(\cos\theta) e^{\pm i m \phi}$, where $P_l^m(\cos\theta)$ are associated Legendre polynomials, which satisfy the equation

$$L^2 Y_l^m(\theta, \phi) = l(l+1) Y_l^m(\theta, \phi) \tag{23}$$

for $l, m = 1, 2, 3, \ldots$ and the unknown temporal exponent σ is in general complex. Substituting these solutions into equations (7) and (5) we obtain the governing equations

$$\left(\frac{d^2}{dr^2} + \frac{2}{r}\frac{d}{dr} - \frac{l(l+1)}{r^2}\right)\left(\frac{d^2}{dr^2} + \frac{2}{r}\frac{d}{dr} - \frac{l(l+1)}{r^2} - \frac{\sigma}{P_r}\right) w = 0, \tag{24}$$

$$\left(\frac{d^2}{dr^2} + \frac{2}{r}\frac{d}{dr} - \frac{l(l+1)}{r^2} - \sigma\right) T + \frac{\alpha}{r^3} w = 0, \tag{25}$$

and the boundary conditions

$$\sigma F - \frac{w}{r} = 0, \tag{26}$$

$$\frac{d}{dr}\left[r\left(\frac{d^2}{dr^2} - \frac{3l(l+1)}{r^2} - \frac{\sigma}{P_r}\right) w\right] + \frac{(2 - l(l+1))}{r^2}\left[2w + \frac{l(l+1)F}{C_r}\right] = 0, \tag{27}$$

$$\left[\frac{d^2}{dr^2} - \frac{(2 - l(l+1))}{r^2}\right] w + \frac{M l(l+1)}{r}\left(T - \frac{\alpha F}{r^2}\right) = 0, \tag{28}$$

$$\frac{dT}{dr} + \frac{2\alpha F}{r^3} + B_i\left(T - \frac{\alpha F}{r^2}\right) = 0, \tag{29}$$

evaluated on $r = r_2$ and

$$w = 0, \tag{30}$$

$$\frac{dw}{dr} = 0, \tag{31}$$

together with either

$$T = 0 \quad \text{or} \quad \frac{dT}{dr} = 0 \tag{32}$$

evaluated on $r = r_1$. Notice that we have used equation (18) to eliminate M from equation (13) to obtain equation (27).

4.1. The Planar Limit

An important check on the correctness of the above formulation is that in the limit $r_1 \to \infty$ we should recover the equations and boundary conditions in the case of a planar layer of thickness d. We write $r = r_1 + z$ so that the undisturbed layer lies between $z = 0$ and $z = 1$ and as $r_1 \to \infty$ then $w(r) \sim r_1 W(z)$, $T(r) \sim T(z)$, $\alpha \sim r_1^2$ and $l(l+1) \sim r_1^2 a^2$, where a is the wave number in the plane. In this limit we obtain the equations

$$\left(\frac{d^2}{dz^2} - a^2\right)\left(\frac{d^2}{dz^2} - a^2 - \frac{\sigma}{P_r}\right) W = 0, \tag{33}$$

$$\left(\frac{d^2}{dz^2} - a^2 - \sigma\right) T + W = 0, \tag{34}$$

and the boundary conditions

$$\sigma F - W = 0, \tag{35}$$

$$\frac{d}{dz}\left(\frac{d^2}{dz^2} - 3a^2 - \frac{\sigma}{P_r}\right) W - \frac{a^4 F}{C_r} = 0, \tag{36}$$

$$\left(\frac{d^2}{dz^2} + a^2\right) W + a^2 M(T - F) = 0, \tag{37}$$

$$\frac{dT}{dz} + B_i(T - F) = 0 \tag{38}$$

evaluated on $z = 1$, and $W = dW/dz = 0$ together with either $T = 0$ or $dT/dz = 0$ evaluated on $z = 0$. This formulation is in exact agreement with that given by Takashima [14,15] for the onset of Marangoni convection in a planar layer in the absence of gravity.

4.2. Comparison with Cloot & Lebon [2]

At this point we observe that the above boundary conditions differ from those presented by Cloot & Lebon [2] for the same problem. The most significant difference between their work and the present one is their equation (3.9), which should correspond to our equation (27). Rather than using the operator L^2 to differentiate the boundary condition (11) *along* $r = r_2$ as

we have done Cloot & Lebon [2] apparently differentiated it with respect to r *across* $r = r_2$ and then substituted for

$$\frac{\partial P_1}{\partial r} = \frac{P_r}{r}\left(\nabla^2 - \frac{1}{P_r}\frac{\partial}{\partial t}\right)(ru_r)$$

from the r-component of the governing equation (4). Not surprisingly, since the boundary condition (11) only holds on $r = r_2$ and not across it, their resulting boundary condition (3.9) is incorrect. There are three other more minor differences. Equation (2.11) of their paper, corresponding to the present equation (9), has an extra factor of $1/P_r$ multiplying the term $\partial F/\partial t$. However, since the authors only consider the onset of steady convection this error has no effect on the results presented. Their equation (3.8), corresponding to the present equation (28), has an extra factor of 2 multiplying the term $\alpha F/r^2$ arising from the first order perturbation in T_0 caused by the deflection of the free surface. Their equation (3.10), corresponding to the present equation (29), omits the term $2\alpha F/r^3$ arising from the first order perturbation in $\partial T_0/\partial r$ caused by the deflection of the free surface. Notice that as a consequence of these errors Cloot & Lebon's [2] boundary conditions do *not* reduce to those for the plane case in the limit $r_1 \to \infty$. None of these errors affect the special case $C_r = 0$ treated by Pirotte & Lebon [9,10] but obviously the interesting new behaviour described by Cloot & Lebon [2] in the case $C_r \neq 0$ must be re-examined.

5. The onset of steady convection

In the remainder of this work we shall consider only the onset of steady convection characterised by $\sigma = 0$, and in this special case the equations and boundary conditions (24) - (32) become

$$\left(\frac{d^2}{dr^2} + \frac{2}{r}\frac{d}{dr} - \frac{l(l+1)}{r^2}\right)^2 w = 0, \tag{39}$$

$$\left(\frac{d^2}{dr^2} + \frac{2}{r}\frac{d}{dr} - \frac{l(l+1)}{r^2}\right) T + \frac{\alpha}{r^3} w = 0, \tag{40}$$

together with

$$w = 0, \tag{41}$$

$$\frac{d}{dr}\left[r\left(\frac{d^2}{dr^2} - \frac{3l(l+1)}{r^2}\right) w\right] - \frac{l(l+1)(l-1)(l+2)F}{r^2 C_r} = 0, \tag{42}$$

$$\frac{d^2 w}{dr^2} + \frac{Ml(l+1)}{r}\left(T - \frac{\alpha F}{r^2}\right) = 0, \tag{43}$$

$$\frac{dT}{dr} + \frac{2\alpha F}{r^3} + B_i\left(T - \frac{\alpha F}{r^2}\right) = 0, \tag{44}$$

evaluated on $r = r_2$ and

$$w = 0, \tag{45}$$

$$\frac{dw}{dr} = 0, \tag{46}$$

together with either

$$T = 0 \quad \text{or} \quad \frac{dT}{dr} = 0 \tag{47}$$

evaluated on $r = r_1$.

6. Solution for Steady Convection

Equations (39) and (40) have the general solutions

$$w(r) = A_1 r^l + A_2 r^{l+2} + A_3 r^{-(l+1)} + A_4 r^{-(l-1)}, \tag{48}$$

$$T(r) = B_1 r^{l-1} + B_2 r^{l+1} + B_3 r^{-(l+2)} + B_4 r^{-l} + B_5 r^l + B_6 r^{-(l+1)}, \tag{49}$$

where

$$A_1 = \frac{2lB_1}{\alpha}, \quad A_2 = -\frac{2(l+1)B_2}{\alpha}, \quad A_3 = -\frac{2(l+1)B_3}{\alpha}, \quad A_4 = \frac{2lB_4}{\alpha}.$$

If we solve equation (42) for the free surface deflection then we obtain

$$F = \frac{r^2 C_r}{l(l+1)(l-1)(l+2)} \frac{d}{dr}\left[r\left(\frac{d^2}{dr^2} - \frac{3l(l+1)}{r^2}\right) w\right] \tag{50}$$

evaluated on $r = r_2$, provided that $l(l+1)(l-1)(l+2) \neq 0$, i.e. $l \neq -2, -1, 0, 1$. The six unknowns $B_1, \ldots, B_6$ are then determined by the remaining six boundary conditions. The dispersion relationship between M, l, C_r, B_i and r_1 is determined by substituting the general solutions into the boundary conditions and evaluating the resulting determinant of the coefficients of the unknowns, which can be written in the form $D_1 + MD_2 = 0$, where D_1 and D_2 are two 6×6 determinants which are independent of M. In fact it is easy to show that D_1 is also independent of C_r and D_2 of B_i and hence that on the marginal stability curves M has the functional form

$$M = \frac{\alpha(l, r_1) + \beta(l, r_1) B_i}{1 + \gamma(l, r_1) C_r}, \tag{51}$$

where $\alpha(l, r_1)$, $\beta(l, r_1)$ and $\gamma(l, r_1)$ are functions of l and r_1. In practice the calculation of M was performed in two different ways. The first method was to use the MAPLE computer algebra package running on a SUN SPARCstation to solve the equations subject to the boundary conditions directly. The analytical expressions of the functions $\alpha(l, r_1)$, $\beta(l, r_1)$ and $\gamma(l, r_1)$ were obtained this way but, since they are rather too complicated to be useful, they are not repeated here. The second method was to use a FORTRAN program employing the NAG routine F03ADF and running on a VAX mainframe to evaluate D_1 and D_2 numerically and hence calculate $M = -D_1/D_2$. In all the cases considered both methods gave exactly the same answers to within the bounds of numerical error and the analytical and numerical results obtained are presented in the following section.

7. Results

7.1. The Marginal Stability Curves

The marginal stability curves in the (l, M) plane on which $\sigma = 0$ are given by $M = M(l, C_r, B_i, r_1)$ and separate regions of unstable modes with $\Re(\sigma) > 0$ from those of stable

modes with $\Re(\sigma) < 0$, where $\Re(\cdot)$ denotes the real part of a complex quantity. In all the cases considered the portion of the (l, M) plane lying above the marginal stability curves in the half-plane $M > 0$ and the portion lying below them in $M < 0$ (if any) correspond to unstable modes and so we can calculate a minimum and a maximum critical Marangoni number, denoted by $M = M_c^+(C_r, B_i, r_1)$ and $M = M_c^-(C_r, B_i, r_1)$ respectively with corresponding critical wave numbers $l = l_c^+(C_r, B_i, r_1)$ and $l = l_c^-(C_r, B_i, r_1)$, such that disturbances with Marangoni numbers lying in the range $M_c^- < M < M_c^+$ are linearly stable to steady convection. Notice that although we can calculate the marginal stability curves for all real values of l only those values of M for integer values of $l = 1, 2, \ldots$ correspond to physically realisable situations, and the task of calculating M_c^+, l_c^+ and M_c^-, l_c^- is simply that of finding the appropriate minimum and maximum values of M for integer values of $l = 1, 2, \ldots$.

7.2. Non-deformable Free Surface

In the special case $C_r = 0$, corresponding to the asymptotic limit of large surface tension, the free surface is non-deformable so that $F = 0$ and the boundary conditions (43) and (44) simplify to give

$$\frac{d^2w}{dr^2} + \frac{Ml(l+1)}{r}T = 0, \tag{52}$$

$$\frac{dT}{dr} + B_i T = 0 \tag{53}$$

evaluated on $r = r_2$ in agreement with the formulations of Pirotte & Lebon [9,10] and Hoefsloot & Hoogstraten [5].

Typical numerically calculated marginal stability curves when $C_r = 0$ are shown in Figure 1 for a range of values of B_i when $r_1 = 1$ in both conducting and insulating cases. Note again that although we have plotted the marginal stability as a continuous function of l only the points corresponding to integer values of $l = 1, 2, \ldots$ (marked with a dot) correspond to physically realisable situations. When $C_r = 0$ the marginal stability curves always lie in the half-plane $M > 0$ so that $M_c^- = -\infty$ and l_c^- is undefined, which means that all situations with $M < 0$ are always stable while those with $M > 0$ are stable only if $M < M_c^+$. The curves in Figure 1 also illustrate that the different thermal boundary conditions at the inner boundary affect the long wavelength ($l \to 0$) behaviour of the curves. In fact we can solve the appropriate leading order problems to show that as $l \to 0$ then in the conducting case

$$M \sim \frac{1}{l}\frac{(r_1 + r_2 B_i)}{r_1 f_1}, \tag{54}$$

while in the insulating case

$$M \sim \frac{1}{r_2^2 f_2} \tag{55}$$

if $B_i = 0$ and

$$M \sim \frac{1}{l}\frac{B_i}{f_2} \tag{56}$$

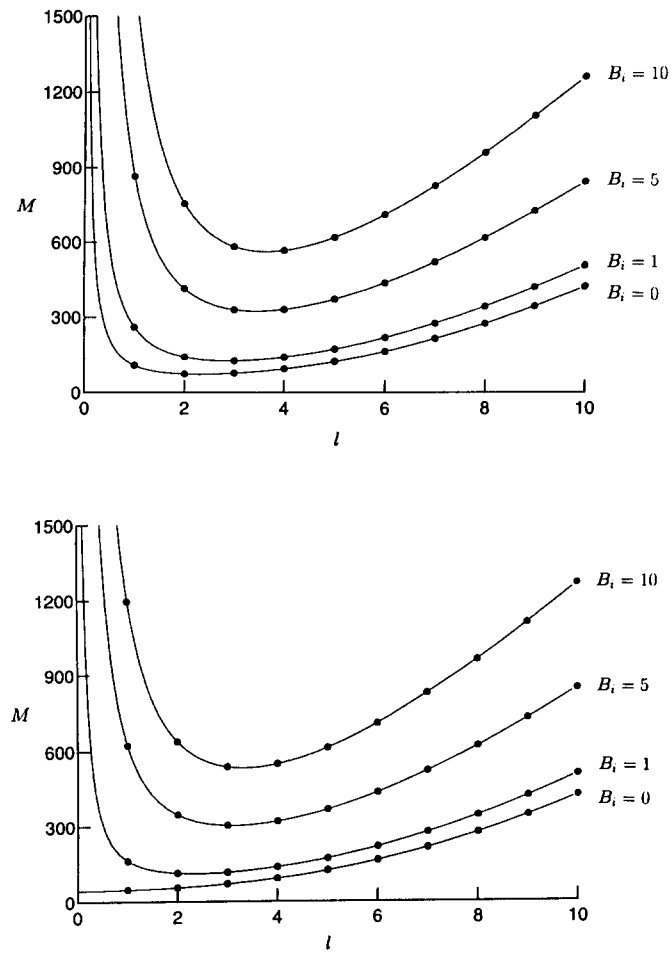

Fig. 1. Numerically computed marginal stability curves plotted as functions of $l \geq 0$ when $C_r = 0$ and $r_1 = 1$ for a range of values of B_i in (a) the conducting case (b) the insulating case. The points corresponding to integer values of $l = 1, 2, \ldots$ are marked with a dot (•).

if $B_i \neq 0$, where the functions f_1 and f_2 are given by

$$f_1 = \frac{r_2}{4(r_1 + r_2)} \left[r_2^3 + 9r_1 r_2 - r_1^3 + 6(r_1 + r_2) r_1 r_2 \ln\left(\frac{r_1}{r_2}\right) \right], \tag{57}$$

$$f_2 = \frac{r_1}{4(r_1 + r_2)} \left[r_2^2 + 4r_1 r_2 - 5r_1^2 + 2r_1(r_1 + 2r_2) \ln\left(\frac{r_1}{r_2}\right) \right]. \tag{58}$$

In the opposite limit of short wavelength disturbances ($l \to \infty$) then we can again solve the appropriate leading order problem to show that

$$M \sim \frac{4(2l + 1)(l + r_2 B_i)}{r_1 r_2} \tag{59}$$

as $l \to \infty$, regardless of the thermal boundary condition at the inner boundary.

Typical numerically calculated values of M_c^+ and l_c^+ are shown in Table 1 for a range of values of B_i and r_1 in both conducting and insulating cases. Table 2 shows numerically

Table 1. Numerically calculated values of M_c^+ and l_c^+ when $C_r = 0$ for a range of values of B_i and r_1 in both conducting and insulating cases. In the limit $B_i \to \infty$ the limiting value of M_c^+/B_i rather than M_c^+ is given.

		Conducting		Insulating	
r_1	B_i	M_c^+	l_c^+	M_c^+	l_c^+
1	0	73.4957	2	47.2500	1
1	1	127.5290	3	113.2931	2
1	5	329.3507	3	302.6425	3
1	10	566.5070	4	536.1769	3
1	∞	47.1743	4	45.5806	4
5	0	76.6182	10	46.0369	1
5	1	116.8962	12	98.3159	9
5	5	264.3068	14	241.9132	12
5	10	443.1586	15	412.6841	13
5	∞	35.2312	16	33.5765	15
10	0	77.9130	20	46.8102	1
10	1	116.3334	23	97.1438	18
10	5	257.3266	27	234.7074	24
10	10	428.1877	28	397.9382	25
10	∞	33.6644	31	32.0452	28

calculated values of M_c^+, $\partial M_c^+/\partial B_i$ and l_c^+ in the case $r_1 = 15$ for a range of values of B_i in the conducting case and demonstrates that, in agreement with the functional form given in equation (51), M_c^+ is a piecewise linear increasing function of B_i with the discontinuities in $\partial M_c^+/\partial B_i$ corresponding to the discontinuous jumps between integer values of l_c^+.

Figure 2(a) and Figure 2(b) show the behaviour of the computed values of M_c^+ and $(l_c^+(l_c^+ + 1))^{\frac{1}{2}}/r_1$ plotted as functions of r_1 when $B_i = 0$ in the conducting case and demonstrate how the solution in the planar case is recovered in the limit $r_1 \to \infty$ in which $M_c^+ \sim 79.607$ and $(l_c^+(l_c^+ + 1))^{\frac{1}{2}}/r_1 \sim 1.99$. The oscillations in M_c^+ are shown in greater detail in Figure 2(c). Note that the discontinuities in $\partial M_c^+/\partial r_1$ correspond to the discontinuous jumps between integer values of l_c^+. The oscillations in M_c^+ and associated discontinuities in l_c^+ occur because the symmetry constraints of the spherical geometry mean that the fluid has only a discrete set of possible modes and neither occur in the planar limit $r_1 \to \infty$ when a continuum of possible modes is available.[1]

7.3. Deformable Free Surface

In the general case $C_r \neq 0$ the free surface is deformable and, as we shall see, this has a dramatic effect on the stability characteristics of the layer.

[1] For the same reason similar results have recently been obtained numerically by Lebon & Dauby [6] for the onset of steady Marangoni convection in a finite-sized rectangular box with a non-deformable free surface which also approach the values in the planar case as the lateral dimensions of the box are increased.

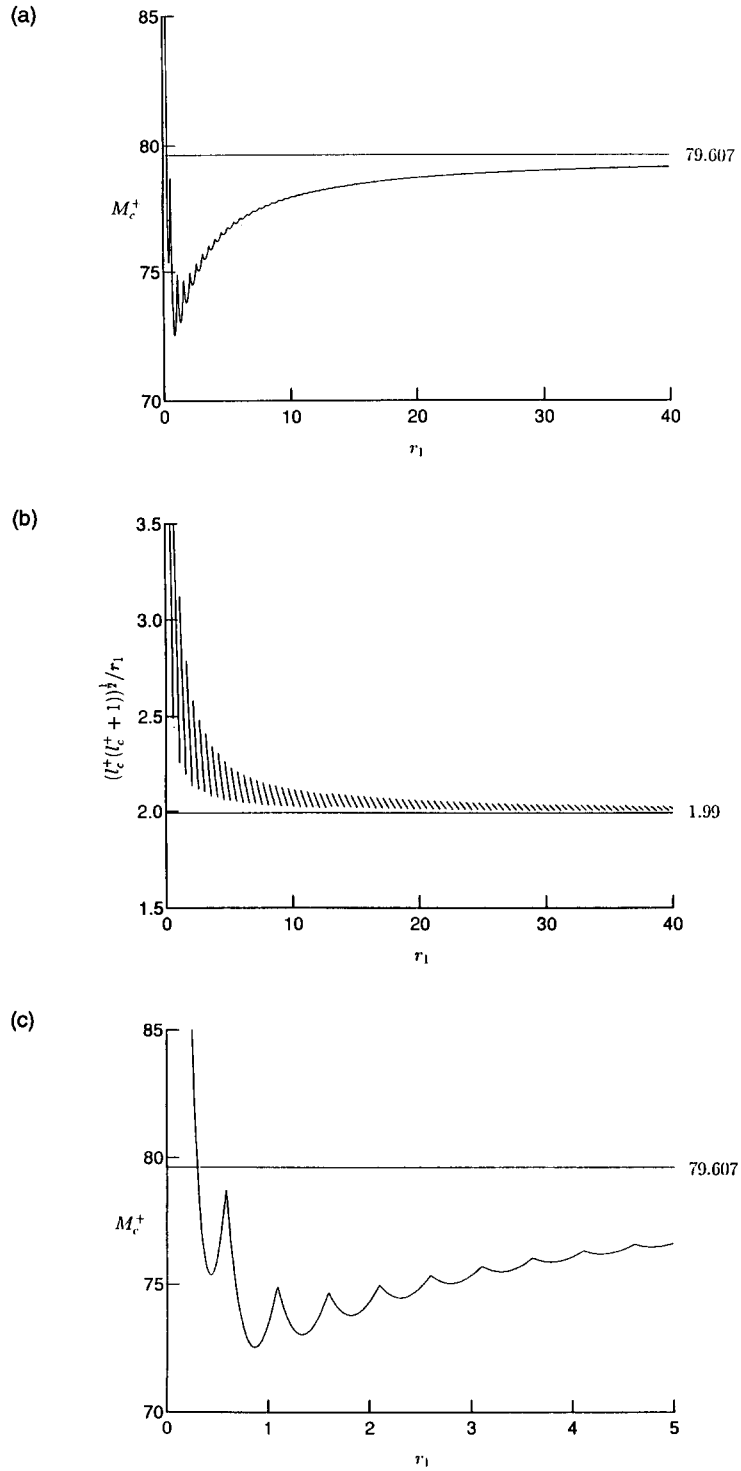

Fig. 2. Numerically computed values of (a) M_c^+ and (b) $(l_c^+(l_c^+ + 1))^{\frac{1}{2}}/r_1$ plotted as functions of r_1 in the conducting case when $C_r = 0$ and $B_i = 0$; (c) shows the first part of the curve for M_c^+ in greater detail.

Table 2. Numerically calculated values of M_c^+, $\partial M_c^+/\partial B_i$ and l_c^+ when $C_r = 0$ in the case $r_1 = 15$ for a range of values of B_i in the conducting case demonstrating that M_c^+ is an increasing piecewise linear function of B_i.

B_i	M_c^+	$\partial M_c^+/\partial B_i$	l_c^+
0	78.4280	40.2018	30
1	116.2324	36.5994	34
2	151.9278	34.9272	37
3	186.6956	34.5179	38
4	221.0172	34.1718	39
5	255.0517	33.8835	40
6	288.9352	33.8835	40
7	322.5894	33.6483	41
8	356.2378	33.6483	41
9	389.7369	33.4621	42
10	423.1990	33.4621	42

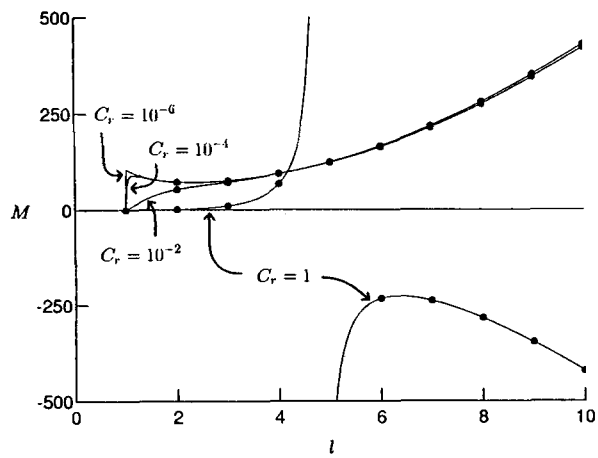

Fig. 3. Numerically computed marginal stability curves plotted as functions of $l \geq 1$ when $B_i = 0$ and $r_1 = 1$ for a range of non-zero values of $C_r = 10^{-6}, 10^{-4}, 10^{-2}$ and 1 in the conducting case. The points corresponding to integer values of $l = 1, 2, \ldots$ are marked with a dot (•).

Typical numerically calculated marginal stability curves for a range of values of $C_r \neq 0$ are shown in Figure 3 when $B_i = 0$ and $r_1 = 1$ in the conducting case. The curves shown in Figure 3 are dramatically different from those in the case $C_r = 0$ shown in Figure 1, firstly because they all take the value $M = 0$ at $l = 1$ and secondly because for sufficiently large values of C_r they extend into the half-plane $M < 0$.

As we can see from equation (50) when $C_r \neq 0$ the case $l = 1$ requires special attention. In this case we can solve equation (44) for F and then use the remaining boundary conditions

to solve for the unknowns $B_1, \ldots, B_6$. However, if we do this we find that when $M \neq 0$ then only the trivial solution $B_1 = \ldots = B_6 = 0$ is possible, while if $M = 0$ then there is a non-trivial solution given by $B_1 = \ldots = B_4 = 0$ and $B_6 = -r_1^3 B_5$ in the conducting case or $B_6 = r_1^3 B_5/2$ in the insulating case. We are therefore forced to conclude that $M = 0$ at $l = 1$ when $C_r \neq 0$ regardless of the other parameters and the thermal boundary conditions at the inner boundary. In all the cases considered this is the minimum value of the marginal stability curves in $M > 0$ and so $M_c^+ = 0$ at $l_c^+ = 1$ which means that, in sharp contrast to the case $C_r = 0$, all the situations with $M > 0$ are always unstable.

In the limit of short wavelength disturbances ($l \to \infty$) we can solve the appropriate leading order problem to show that

$$M \sim \frac{4(2l+1)(l+r_2 B_i)}{r_1(r_2 - 4C_r)} \tag{60}$$

as $l \to \infty$, regardless of the thermal boundary condition at the inner boundary. This result shows that if $C_r < r_2/4$ then $M \to +\infty$ as $l \to \infty$ and the entire marginal stability curve lies in $M > 0$ as shown in Figure 3 in the cases $C_r = 10^{-6}$, 10^{-4} and 10^{-2}. Hence $M_c^- = -\infty$ and l_c^- is undefined so that all situations with $M < 0$ are stable. However, if $C_r > r_2/4$ then $M \to -\infty$ as $l \to \infty$ and the marginal stability curves extend into $M < 0$ as shown in Figure 3 in the case $C_r = 1$. In this case a finite (negative) value of M_c^- exists and situations with $M < 0$ are stable only if $M > M_c^-$.

Typical numerically calculated values of M_c^- and l_c^- are shown in Table 3 for a range of values of B_i and r_1 in both conducting and insulating cases. Table 4 shows numerically calculated values of M_c^-, $\partial M_c^-/\partial B_i$ and l_c^- in the case $r_1 = 1$ for a range of values of B_i in the conducting case and demonstrates that, in agreement with the functional form given in equation (51), M_c^- is a piecewise linear decreasing function of B_i with the discontinuities in $\partial M_c^-/\partial B_i$ corresponding to the discontinuous jumps between integer values of l_c^-.

Figure 4(a) and Figure 4(b) show the behaviour of the computed values of M_c^- and $(l_c^-(l_c^- + 1))^{\frac{1}{2}}/r_1$ plotted as functions of r_1 when $B_i = 0$ in the conducting case; they demonstrate how the solution in the planar case is recovered in the limit $r_1 \to \infty$ in which $M_c^- = -\infty$ and l_c^- is undefined. The oscillations in M_c^+ are shown in greater detail in Figure 4(c). Just as in the case $C_r = 0$ the discontinuities in $\partial M_c^-/\partial r_1$ correspond to the discontinuous jumps between integer values of l_c^-.

7.4. Physical Mechanisms

A planar layer of fluid is always stable to steady Marangoni convection when heated from above and in order to understand why the behaviour is different in a spherical geometry we have to think a little about the physical mechanisms involved.

The basic mechanism for steady Marangoni convection is described, for example by Davis [3], as follows. Suppose a disturbance creates a hot spot at a point P on the free surface. Since $\gamma > 0$ surface tension decreases with temperature so there is a net surface traction away from P which, since the fluid is viscous, drags fluid below the free surface away from P. Conservation of mass creates an upflow beneath P. If the basic temperature profile of the layer is warmer inside the free surface than at it then this upflow brings warmer fluid towards P. This mechanism is sufficient to create steady convection if the Marangoni number is large enough. Alternatively, if the basic temperature profile of the layer is cooler inside the free surface than at it then this upflow brings cooler fluid towards P which will tend to damp

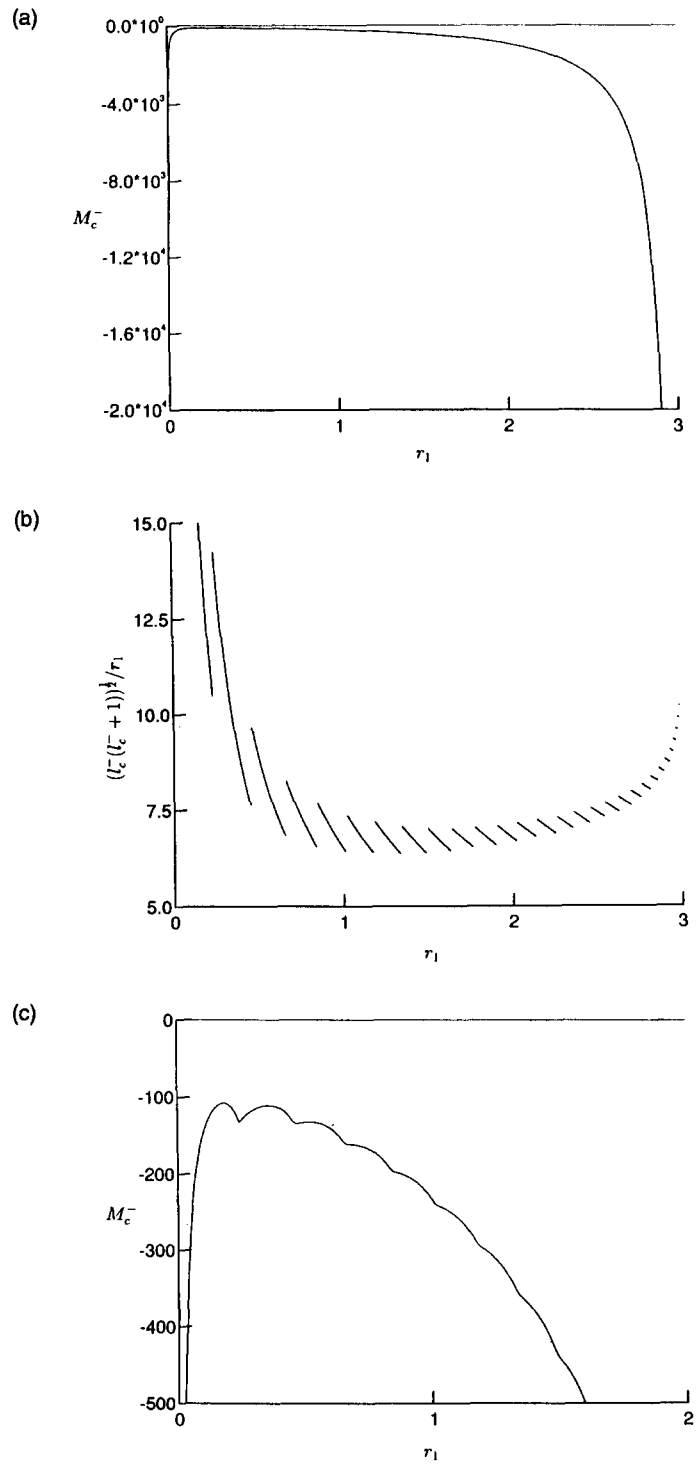

Fig. 4. Numerically computed values of (a) M_c^- and (b) $(l_c^-(l_c^- + 1))^{\frac{1}{2}}/r_1$ plotted as functions of r_1 in the conducting case when $C_r = 1$ and $B_i = 0$; (c) shows the first part of the curve for M_c^- in greater detail.

Table 3. Numerically calculated values of M_c^- and l_c^- when $C_r = 1$ for a range of values of B_i and r_1 in both conducting and insulating cases. In the limit $B_i \to \infty$ the limiting value of M_c^-/B_i rather than M_c^- is given. When $r_1 > 4C_r - 1 = 3$ then $M_c^- = -\infty$ and l_c^- is undefined.

		Conducting		Insulating	
r_1	B_i	M_c^-	l_c^-	M_c^-	l_c^-
1	0	–233.5978	6	–235.5260	6
1	1	–307.7626	7	–308.4760	7
1	5	–581.3155	7	–582.6892	7
1	10	–923.2566	7	–925.4556	7
1	∞	–68.3882	7	–68.5533	7
2	0	–915.9994	13	–920.8942	13
2	1	–1127.3761	13	–1132.8339	14
2	5	–1927.6703	14	–1932.4914	14
2	10	–2924.7334	14	–2932.0632	14
2	∞	–199.4126	14	–199.9144	14

Table 4. Numerically calculated values of M_c^-, $\partial M_c^-/\partial B_i$ and l_c^- when $C_r = 1$ in the case $r_1 = 1$ for a range of values of B_i in the conducting case demonstrating that M_c^- is a decreasing piecewise linear function of B_i.

B_i	M_c^-	$\partial M_c^-/\partial B_i$	l_c^-
0	–233.598	77.8453	6
1	–307.763	68.3882	7
2	–376.151	68.3882	7
3	–444.539	68.3882	7
4	–512.927	68.3882	7
5	–581.316	68.3882	7
6	–649.704	68.3882	7
7	–718.092	68.3882	7
8	–786.480	68.3882	7
9	–854.868	68.3882	7
10	–923.257	68.3882	7

out the the hot spot and so stabilise the layer. Clearly this mechanism is most effective when $B_i = 0$, since when $B_i \neq 0$ some heat is lost to the surrounding passive gas leaving less to generate surface tension gradients. In the limit $B_i \to \infty$ the free surface is isothermal and thermocapillary effects are entirely absent.

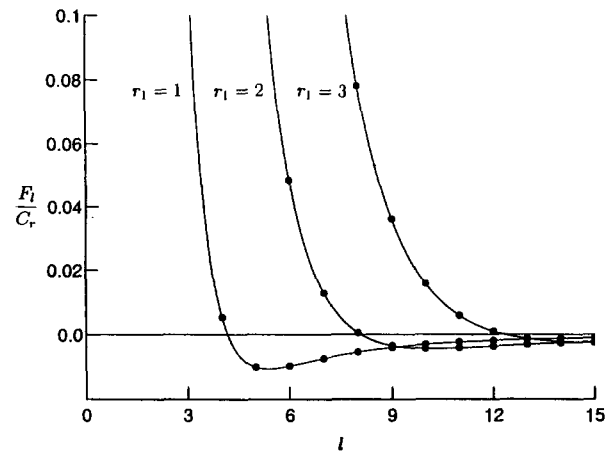

Fig. 5. Numerically computed values of F_l/C_r, defined by equation (61), plotted as functions of $l \geq 1$ when $r_1 = 1, 2$ and 3.

This basic mechanism is independent of the deflection of the free surface and describes the situation when $C_r = 0$. If $C_r \neq 0$ then the deflection of the free surface can have either a stabilising or destabilising influence on the layer. If the basic temperature profile of the layer is warmer inside the free surface than outside it then if the free surface is depressed over the upflow at P then it helps to warm the hot spot, while if the free surface is elevated over the upflow at P then it helps to cool the hot spot. Alternatively, if the basic temperature profile of the layer is cooler inside the free surface than outside it then if the free surface is depressed over the upflow at P then it helps to cool the hot spot, while if the free surface is elevated at P then it helps to warm the hot spot.

In a planar layer currents flowing towards the free surface are *always* accompanied by depressions of the free surface which means that if the layer is heated from below then it may or may not be unstable but the effect of the free surface deflection is always a destabilising one, while if the layer is heated from above then the layer is always stable. In contrast in a spherical geometry we shall see that both elevations and depressions of the free surface over a current flowing towards the free surface are possible, and so when the free surface is deformable the layer can be unstable when heated from either above or below.

One way to show this is to consider the sign of the so-called "flow indicator", F_l, introduced by Scriven & Sternling [12] and Sarma [11] for the planar problem and defined to be

$$F_l = F\left[\frac{du_r}{dr}\right]^{-1} = F\left[\frac{d}{dr}\left(\frac{w}{r}\right)\right]^{-1} \tag{61}$$

evaluated at $r = r_2$. Since $u_r = 0$ at $r = r_2$ if $du_r/dr > 0$ at $r = r_2$ then $u_r < 0$ just below the free surface while if $du_r/dr < 0$ at $r = r_2$ then $u_r > 0$ just below the free surface and so if F_l is *positive* then u_r and F are of *different* signs just below the free surface which means that currents flowing towards the free surface are associated with depressions and while if F_l is *negative* then u_r and F are of the *same* sign just below the free surface which means that currents flowing towards the free surface are associated with elevations. Note that F_l/C_r

depends on l and r_1, but not the thermal boundary conditions. In the planar case we can easily obtain

$$F_l = \frac{2C_r}{\cosh^2 a - 1 - a^2} > 0 \tag{62}$$

and so rising currents near the free surface are *always* associated with depressions of the free surface. In the spherical case the expression for F_l is rather more complicated and so it is not reproduced here, but typical values of F_l/C_r are plotted in Figure 5 as a function of l for $r_1 = 1, 2$ and 3. Figure 5 clearly shows that F_l is positive as $l \to 1^+$ and negative as $l \to \infty$, and so the effect of a deformable free surface can be destabilising when the layer is heated from the outside as well as when it is heated from the inside. In fact we can show that the limiting behaviour of F_l is

$$F_l \sim \frac{r_1 r_2^2 (2r_1^3 + 4r_1^2 r_2 + 6r_1 r_2^2 + 3r_2^3) C_r}{(l-1)(4r_1^2 + 7r_1 r_2 + 4r_2^2)} > 0 \tag{63}$$

as $l \to 1^+$ and

$$F_l \sim -\frac{r_2^2 C_r}{l(l+1)(l+2)} < 0 \tag{64}$$

as $l \to \infty$. Notice that although F_l is always negative as $l \to \infty$ we already know that the layer is unstable when heated from the outside only if $C_r > r_2/4$.

8. Conclusions

In this paper we have used a combination of analytical and numerical techniques to analyse the onset of steady Marangoni convection in a spherical shell of fluid with an outer free surface surrounding a rigid sphere. In so doing we have corrected the formulation of the problem and the results presented by Cloot & Lebon [2]. If the free surface of the layer is non-deformable then the layer is always stable when heated from the outside and is unstable when heated from the inside if the magnitude of the (positive) Marangoni number is sufficiently large. If the free surface of the layer is deformable then the layer is always unstable when heated from the inside. It is stable when heated from the outside if $C_r < r_2/4$, but if $C_r > r_2/4$ then it is unstable if the magnitude of the (negative) Marangoni number is sufficiently large.

Acknowledgement

The author is very grateful to Dr B.R. Duffy (University of Strathclyde) for his assistance.

References

1. S. Chandrasekhar, *Hydrodynamic and Hydromagnetic Stability.* OUP (1961).
2. A. Cloot and G. Lebon, Surface deformation effect on Marangoni convection in a spherical shell. *Microgravity sci. technol.* **3** (1) (1990) 44–46.
3. S.H. Davis, Thermocapillary instabilities. *Ann. Rev. Fluid Mech.* **19** (1987) 403–435.
4. G. Gouesbet, J. Maquet, C. Rozé, and R. Darrigo, Surface-tension and coupled buoyancy-driven instability in a horizontal liquid layer. Overstability and exchange of stability. *Phys. Fluids A* **2** (6) (1990) 903–911.
5. H.C.J. Hoefsloot and H.W. Hoogstraten, Marangoni instability in spherical shells. *Appl. microgravity tech.* **2** (2) (1989) 106–108.

6. G. Lebon and P.C. Dauby, Surface-tension driven convection in finite-size containers. ESA-SP 333 (Abstracts) (1992) pp. 52–53.
7. G. Lebon, P.C. Dauby, and A. Cloot, Some problems raised by Marangoni instability in spherical geometry. In *Microgravity Fluid Dynamics*, ed. H.J. Rath, Springer-Verlag (1992) pp. 71–79.
8. J.R.A. Pearson, On convection cells induced by surface tension. *J. Fluid Mech.* **4** (1958) 489–500.
9. O. Pirotte and G. Lebon, Surface-tension driven instability in spherical shells. *Appl. microgravity tech.* **1** (4) (1988) 175–179.
10. O. Pirotte and G. Lebon, Comments on the paper 'Marangoni instability in spherical shells'. *Appl. microgravity tech.* **2** (2) (1989) 108–109.
11. G.S.R. Sarma, Interactions of surface-tension and buoyancy mechanisms in horizontal liquid layers. *J. Thermophys.* **1** (2) (1987) 129–135.
12. L.E. Scriven and C.V. Sternling, On cellular convection driven by surface-tension gradients: effects of mean surface tension and surface viscosity. *J. Fluid Mech.* **19** (1964) 321–340.
13. K.A. Smith, On convective instability induced by surface-tension gradients. *J. Fluid Mech.* **24** (1966) 401–414.
14. M. Takashima, Surface tension driven instability in a horizontal liquid layer with a deformable free surface. I. Steady Convection. *J. Phys. Soc. Japan* **50** (8) (1981) 2745–2750.
15. M. Takashima, Surface tension driven instability in a horizontal liquid layer with a deformable free surface. II. Overstability. *J. Phys. Soc. Japan* **50** (8) (1981) 2751–2756.